

Generalized Onsager's Relation in Magnon Hall Effect and Its Implication

Jikun Zhou

CAS Key Laboratory of Strongly-Coupled Quantum Matter Physics and Department of Physics,
University of Science and Technology of China, Hefei, Anhui 230026, China

Yang Gao* and Qian Niu

CAS Key Laboratory of Strongly-Coupled Quantum Matter Physics and Department of Physics,
University of Science and Technology of China, Hefei, Anhui 230026, China and
Hefei National Laboratory, University of Science and Technology of China, Hefei 230088, China

(Dated: January 14, 2025)

By analyzing the spin-group symmetry of magnons, we establish two generalized Onsager's relations in the magnon Hall effect, which reveals the rich and complicated structures of the magnon Berry curvature in the parameter space of different types of the exchange coupling. As an important consequence, we find that the isotropic exchange coupling is equally important as the Dzyaloshinskii-Moriya (DM) interaction in determining the magnon Hall effect, and it can transform to the latter under proper gauge transformation. Moreover, the diagonal and off-diagonal part of the symmetric anisotropic exchange coupling together can support the magnon Hall effect without the DM interaction. Both features are exemplified in ferromagnetic honeycomb lattices. Our work lays the ground for decoding the coupling between magnon transport and different types of exchange interactions.

Introduction.—As potential carriers in energy and spin transport, magnons, elementary excitations of spin orders, have drawn much attention in recent years. One outstanding example is the magnon Hall effect [1–17], which generates a thermal current perpendicular to the applied temperature gradient. The corresponding thermal conductivity can be related to the Berry curvature of magnon in the momentum space [1, 2, 5]. As a fundamental rule, the Onsager's reciprocal relation [18, 19] restricts the structure of the transport coefficient. In the electronic counterpart, i.e., the anomalous Hall effect [20], it enforces the corresponding conductivity to be an odd function of the spin orientation, reveals the intimate relation between the band geometry and the order parameter, and hence serves as a guiding principle for experimental detection. In the magnonic case, however, besides separate case studies, a comprehensive understanding of the Onsager's relation is still missing.

The difficulty lies in the identification of the critical parameter in the magnon transport. It is widely believed that the Dzyaloshinskii-Moriya (DM) interaction [21, 22] serves as an order parameter, associated with the breaking of the effective time-reversal symmetry consisting of a spin rotation and real time-reversal operation [4, 17, 23], so that the thermal Hall conductivity is an odd function of the DM interaction. However, it has been long overlooked that due to the spin-group symmetry, the choice of the spin rotation axis contains large gauge freedom, which essentially mixes the isotropic, anisotropic and antisymmetric part of the exchanging coupling. This complexity has been implicitly envisioned in recent studies which show that the anisotropic exchange coupling [24, 25] may also induce a nontrivial magnon Hall effect [7]. To accurately identify the critical parameter in the magnon Hall effect, a detailed analysis of the effective

time reversal symmetry from the spin-group perspective is required.

In this work, we provide such a theory and derive two generalized Onsager's relations. For any periodic magnetic textures, we use a local formulation of the magnonic Hamiltonian. We then identify the group \tilde{G} of full effective time reversal operations (see Eq. (8)), inherited from the spin-only group [26–33] in the original magnetic lattice. We find two types of effective time reversal operations, i.e., the uniform one and non-uniform one, from which two Onsager's relations are established, revealing the rich and complicated dependence of the magnon Berry curvature on various exchange couplings. As important consequences, we find that the isotropic exchange coupling is as important as the DM interaction in determining the magnon Hall effect, and that the off-diagonal and diagonal part of the anisotropic exchange coupling can replace the role of the isotropic exchange coupling and DM interaction, respectively. Such findings are exemplified in magnons on ferromagnetic honeycomb lattices.

Local formulation of magnons.—We first set up the general framework for discussing the effective time reversal operation and its implication. Without loss of generality, we assume that the spin texture still possesses the lattice translation symmetry and that there can be arbitrary number of spins in a unit cell, each of which can point along different directions in equilibrium. An example of such system is shown in Fig. 1. Instead of choosing a global coordinate system for the spin texture, we adopt the following rule: we define local coordinate systems on different lattice sites such that the z -axis of the local frame always points along the equilibrium direction of the local spin order, as shown in Fig. 1. Due to the periodicity of the spin texture, the local coordinate

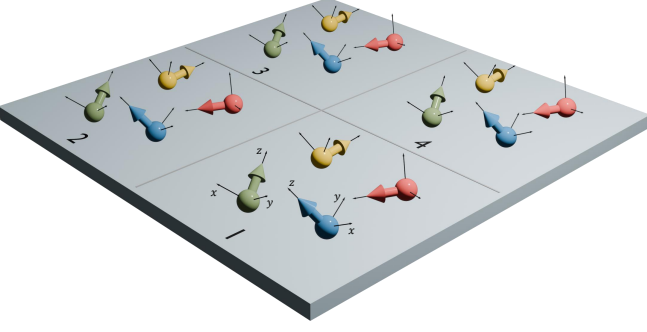


FIG. 1. Configuration of a general magnetic system. Different colors of spins represent different sublattices and spins belong to the same sublattice have same orientation and local coordinate.

frame defined in this way is also periodic.

We now write down the general spin Hamiltonian within this local frame. As the topic in concern is the transport of the spin wave, we focus on the Hamiltonian of the fluctuation around the equilibrium spin texture and ignore how such texture is achieved. For a stable spin texture, it is required that the energy is quadratic and positive with respect to any fluctuation. With this in mind, the spin Hamiltonian should take the following quadratic form:

$$H = \frac{1}{2} \sum_{n,m} \sum_{i,j} \sum_{ab} S_{ni}^a J_{ni,mj}^{ab} S_{mj}^b, \quad (1)$$

where S_{ni}^a is the a -th component of the local spin on the i -th lattice site in the n -th unit cell, and $J_{ni,mj}^{ab}$ contains all exchange interactions between local spins. Moreover, $J_{ni,mj}^{ab} = 0$ when one of the ab indices takes z and the other one takes x or y . For definiteness, we assume that there are N different spins in a unit cell. It is clear that Eq. (1) contains all the quadratic forms of the fluctuation.

We now put the spin Hamiltonian into the canonical form. Through the Fourier transform and the Holstein-Primakoff transformation [34], the spin Hamiltonian can be expressed in the momentum space using the Nambu basis up to a constant: $H = \sum_{\mathbf{k}} \psi_{\mathbf{k}}^\dagger \mathcal{H}_{\mathbf{k}} \psi_{\mathbf{k}}$ with

$$\mathcal{H}_{\mathbf{k}} = \frac{S}{2} \begin{bmatrix} \mathbf{A}(\mathbf{k}) & \mathbf{B}(\mathbf{k}) \\ \mathbf{B}^*(-\mathbf{k}) & \mathbf{A}^*(-\mathbf{k}) \end{bmatrix}. \quad (2)$$

Here $\psi_{\mathbf{k}} = (a_{1,\mathbf{k}}, \dots, a_{N,\mathbf{k}}, a_{1,-\mathbf{k}}^\dagger, \dots, a_{N,-\mathbf{k}}^\dagger)^T$ represent the Nambu basis. The block of Eq. (2) can be expressed by $J_{ni,mj}^{ab}$ [14, 33, 35]

$$A_{ij}(\mathbf{k}) = \sum_{m,n} \frac{1}{2} (J_{ni,mj}^+ - iD_{ni,mj}) e^{i\mathbf{k} \cdot (\mathbf{R}_{mj} - \mathbf{R}_{ni})} - \delta_{ij} \sum_{mnl} J_{ni,m\ell}^{zz}, \quad (3)$$

$$B_{ij}(\mathbf{k}) = \sum_{m,n} \frac{1}{2} (J_{ni,mj}^- + i\Gamma_{ni,mj}) e^{i\mathbf{k} \cdot (\mathbf{R}_{mj} - \mathbf{R}_{ni})}, \quad (4)$$

where \mathbf{R}_{ni} is the position of the i -th spin in the n -th unit cell, $J_{ni,mj}^+ = J_{ni,mj}^{xx} + J_{ni,mj}^{yy}$, $J_{ni,mj}^- = J_{ni,mj}^{xx} - J_{ni,mj}^{yy}$, $D_{ni,mj} = J_{ni,mj}^{xy} - J_{ni,mj}^{yx}$, and $\Gamma_{ni,mj} = J_{ni,mj}^{xy} + J_{ni,mj}^{yx}$. By summing over the unit cell index, we can further define the following symbols according to Eq. (3): $A_{ij} = J_{ij}^+ - iD_{ij} - \delta_{ij} \sum_{mnl} J_{ni,m\ell}^{zz}$ and $B_{ij} = J_{ij}^- + i\Gamma_{ij}$. One can further check that $A(\mathbf{k}) = A^\dagger(\mathbf{k})$ and $B(\mathbf{k}) = B^T(-\mathbf{k})$. As a result, \mathcal{H} is Hermitian.

Interestingly, the definition of the intermediate quantities J^\pm , D and Γ agrees with the decomposition of the exchange coefficient. With fixed lower indices, $J_{ni,mj}^{ab}$ is a rank-2 tensor, which can then be decomposed into three parts in the xy subspace: the scalar part, also referred to as the isotropic exchange interaction, is represented by J^+ , the antisymmetric part, also referred to as the DM interaction, is represented by D , the traceless symmetric part is represented by J^- and Γ . We shall emphasize the $\pi/2$ phase difference between J^+ and D , and J^- and Γ , and the fact that J^+ and D work in the particle or hole sector but J^- and Γ mix particles with holes in the magnon Hamiltonian.

The Hamiltonian in Eq. (2) can be diagonalized by using para-unitary transformation[36–39]

$$T_{\mathbf{k}}^\dagger \mathcal{H}_{\mathbf{k}} T_{\mathbf{k}} = \begin{bmatrix} E_{\mathbf{k}} & \\ & E_{-\mathbf{k}} \end{bmatrix}, \quad (5)$$

where $E_{\mathbf{k}} = \text{diag}(\varepsilon_{1,\mathbf{k}}, \varepsilon_{2,\mathbf{k}}, \dots, \varepsilon_{N,\mathbf{k}})$. The structure of the eigen energy is due to particle-hole symmetry. In order to maintain bosonic commutation rules, the transformation matrix $T_{\mathbf{k}}$ has to satisfy a special orthonormal condition $T_{\mathbf{k}}^\dagger \Sigma_z T_{\mathbf{k}} = \Sigma_z$, where $\Sigma_z = \sigma_z \otimes \mathbb{I}_N$ with σ_z being the Pauli matrix and \mathbb{I}_N being the $N \times N$ unit matrix.

Within this framework, the thermal Hall conductivity of non-interacting magnons is given by [2, 5]

$$\kappa_{\mu\nu} = -\frac{k_B^2 T}{\hbar(2\pi)^2} \sum_{n=1}^N \int_{BZ} c_2[\rho(\varepsilon_{n,\mathbf{k}})] (\Omega_{\mu\nu})_{n,\mathbf{k}} d^2k, \quad (6)$$

where $c_2(\rho) = (1+\rho)(\log \frac{1+\rho}{\rho})^2 - (\log \rho)^2 - 2\text{Li}_2(-\rho)$ with $\text{Li}_2(z)$ being the polylogarithm function, ρ_n is Bose distribution function of the n -th band, and $\Omega_{n,\mathbf{k}}$ is Berry curvature [38]:

$$(\Omega_{\mu\nu})_{n,\mathbf{k}} = i \left[\Sigma_z \frac{\partial T_{\mathbf{k}}^\dagger}{\partial k_\mu} \Sigma_z \frac{\partial T_{\mathbf{k}}}{\partial k_\nu} \right]_{nn}. \quad (7)$$

Generalized Onsager's Relation.—At the heart of the Onsager's relation is the time reversal operation T . In the electronic Hall-type conductivity, on one hand, T connects systems with opposite magnetic order; on the other hand, T flips the sign of the Hall conductivity. The Onsager's relation then states that the Hall conductivity is an odd function of the magnetic order[20, 40].

In the magnonic degree of freedom, however, the situation is quite different. Neither the Hamiltonian of the

fluctuation in Eq. (1) nor the Berry curvature in Eq. (7) can be flipped by the time reversal operation T . Therefore, using T alone cannot offer any useful information about the structure of the magnon Hall conductivity.

A practical generalization is the effective time reversal operation $\mathcal{T} = TC_{2x}^s$ [41, 42] where the rotation only acts on spin and flips the spin order. Since \mathcal{T} can flip both the magnon Berry curvature and the DM interaction, it is usually assumed that the DM interaction plays the role of ‘magnetic order’ and is indispensable in the magnon Hall effect [3, 4, 8–16]. We shall emphasize that in previous study [4, 17, 23], this analysis is applied in ferromagnets and coplanar antiferromagnets where a global C_2 spin rotation axis exists.

In the general setting, a significant issue arises: what is the precise meaning of the C_2 spin rotation axis? For non-coplanar spin textures, there is no global spin rotation axis that can simultaneously flip all the spin orders. The best one can define is the local spin rotation axis that differ site by site, as employed in our framework and illustrated in Fig. 1.

The locally defined spin rotation axis makes prominent an elemental issue, i.e., the gauge freedom in choosing the local spin-x direction. At each site in a unit cell, only the spin-z direction is well defined, and any direction perpendicular to the z -th direction can work equally well as the x direction. The spin-x axis on different sites can have no connection. This gauge freedom should also emerge in ferromagnetic and coplanar antiferromagnetic crystals.

Mathematically, the above issue is related to the spin group of the magnetic crystals. In ferromagnets, the magnetic order is subject to the spin-only group $G = \infty 2'$ [26–33], where C_2 rotation axis is perpendicular to the C_∞ axis (i.e., the direction of the ferromagnetic order). For general spin structures, the spin group obeyed by the magnetic order should at least contain the direct product of the subgroup for each one of the spin in a unit cell

$$\tilde{G} = \bigotimes_{i=1}^N G_i, \quad (8)$$

where $G_i = \infty 2'$ with the axis defined in the local spin frame. We emphasize that more symmetry operations can appear that connect the spin orders on different sites. The group G is just the common subgroup obeyed by any periodic spin textures. Although \tilde{G} has been derived previously [32, 33], its implication in magnon transport is still unclear.

This group structure greatly restricts the magnon Hall effect. To see this, we make a gauge transformation that rotates the spin axis on the i -th site about the local z -axis by an angle ϕ_i with i going through all the local spin orders in a unit cell. As a result, we find that $A_{ij} \rightarrow A_{ij}e^{i(\phi_i - \phi_j)}$ and $B_{ij} \rightarrow B_{ij}e^{i(\phi_i + \phi_j)}$. Since the magnon Hall conductivity should not depend on any spe-

cific choice of ϕ_i , the model parameters $J_{ni,mj}^\pm$, $D_{ni,mj}$ and $\Gamma_{ni,mj}$ should only appear in the form of gauge-independent clusters, the number of which is at least N -less than the total number of parameters in Eq. (2).

Since our goal is to study the Onsager’s relation, we shall focus on the effective time reversal operation in this spin group, i.e., $\mathcal{T}_x = TC_{2x}^s$ and $\mathcal{T}_y = TC_{2y}^s$. Although physically equivalent, the arbitrary substitution of one with the other yields distinct constraints on the model parameters.

We start with choosing \mathcal{T}_x identically on each spin in a unit cell, which is the uniform effective time reversal operation. We emphasize that although the mathematical symbol is the same, \mathcal{T}_x on different spins can involve C_{2x} rotations along different axis in the lattice frame. In the magnon case, the effective time reversal operation \mathcal{T}_x is the spinless-version of the time reversal operation, and can be identified as $\mathcal{T}_x = -K$ where K stands for complex conjugation. We then find that [35] $\mathcal{T}_x \mathcal{H}_{\mathbf{k}}(J_{ij}^+, J_{ij}^-, D_{ij}, \Gamma_{ij}) \mathcal{T}_x^{-1} = \mathcal{H}_{-\mathbf{k}}^*(J_{ij}^+, J_{ij}^-, D_{ij}, \Gamma_{ij}) = \mathcal{H}_{\mathbf{k}}(J_{ij}^+, J_{ij}^-, -D_{ij}, -\Gamma_{ij})$. The last equality holds by directly evaluating the Hamiltonian at $-\mathbf{k}$. By calculating the Berry curvature in the original parameter sets $(J_{ij}^+, J_{ij}^-, D_{ij}, \Gamma_{ij})$ but with the time reversal operator and in the new parameter sets $(J_{ij}^+, J_{ij}^-, -D_{ij}, -\Gamma_{ij})$, respectively, we find that

$$(\Omega_{\mu\nu})_{n,\mathbf{k}}(J_{ij}^\pm, D_{ij}, \Gamma_{ij}) = -(\Omega_{\mu\nu})_{n,-\mathbf{k}}(J_{ij}^\pm, -D_{ij}, -\Gamma_{ij}), \quad (9)$$

We then obtain the first Onsager’s relation [35]:

$$\kappa_{\mu\nu}(J_{ij}^\pm, -D_{ij}, -\Gamma_{ij}) = -\kappa_{\mu\nu}(J_{ij}^\pm, D_{ij}, \Gamma_{ij}). \quad (10)$$

The effective time reversal symmetry can also be chosen in a non-uniform manner. We classify the spins in a unit cell into two groups, such that the time reversal operation on spins in the first group is \mathcal{T}_x while that on spins in the remaining group is \mathcal{T}_y . There are consequently two types of parameters J_{ij}^\pm , D_{ij} , and Γ_{ij} , i.e., those with i and j within the same group, labeled by $J_{ij}^{\pm, \text{intra}}$, D_{ij}^{intra} , and $\Gamma_{ij}^{\text{intra}}$ and those with i and j belonging to different groups, labeled by $J_{ij}^{\pm, \text{inter}}$, D_{ij}^{inter} , and $\Gamma_{ij}^{\text{inter}}$. Since $\mathcal{T}_y = K$, we then find that the total effective time reversal symmetry reads as $\mathcal{T} = (-KI_{n_1}) \oplus (KI_{n_2})$ with n_1 and n_2 being the number of spins in the first and second group, respectively. The effect of \mathcal{T} on the intra-group parameters is the same as in the uniform case, i.e., $J_{ij}^{\pm, \text{intra}} \rightarrow J_{ij}^{\pm, \text{intra}}$, $D_{ij}^{\text{intra}} \rightarrow -D_{ij}^{\text{intra}}$, and $\Gamma_{ij}^{\text{intra}} \rightarrow -\Gamma_{ij}^{\text{intra}}$. Due to the relative minus sign between \mathcal{T}_x and \mathcal{T}_y in \mathcal{T} , the effect on the inter-group parameters is opposite: $J_{ij}^{\pm, \text{inter}} \rightarrow -J_{ij}^{\pm, \text{inter}}$, $D_{ij}^{\text{inter}} \rightarrow D_{ij}^{\text{inter}}$, and $\Gamma_{ij}^{\text{inter}} \rightarrow \Gamma_{ij}^{\text{inter}}$. We can then obtain the second On-

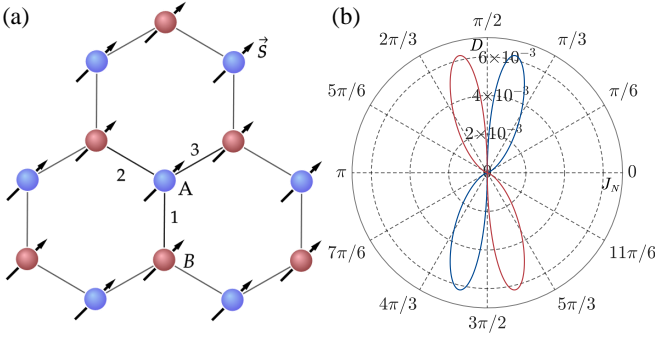


FIG. 2. (a) Honeycomb lattice with in-plane magnetization pointing 45° from the horizontal line. (b) The thermal conductivity as a function of J_N and D . In (b), $J_A = 0.1\sqrt{J_N^2 + D^2}$, $J_B = 0.15\sqrt{J_N^2 + D^2}$; the blue and red curve have positive and negative sign, respectively.

sager's relation[35]:

$$\begin{aligned} \kappa_{\mu\nu}(J_{ij}^{\pm,intra}, -D_{ij}^{intra}, -\Gamma_{ij}^{intra}, -J_{ij}^{\pm,inter}, D_{ij}^{inter}, \Gamma_{ij}^{inter}) \\ = -\kappa_{\mu\nu}(J_{ij}^{\pm,intra}, D_{ij}^{intra}, \Gamma_{ij}^{intra}, J_{ij}^{\pm,inter}, D_{ij}^{inter}, \Gamma_{ij}^{inter}) \end{aligned} \quad (11)$$

The two Onsager's relations in Eq. (10) and (11) are main results of this work. They reveal complicated dependence of the magnon Berry curvature on different types of exchange couplings. The first Onsager's relation can obviously reproduce the usual understanding that the magnon Hall effect is induced by the DM interaction with vanishing anisotropic parameter Γ_{ij} . Besides that, the magnon Hall effect can have much richer structures.

Implications.—One direct consequence of the second Onsager's relation is that the isotropic exchange interaction can be as important as the DM interaction in determining the magnon Hall effect. In fact, the role of the isotropic exchange and that of the DM interaction are even interchangeable by a proper gauge transformation. On one hand, with vanishing anisotropic exchange coupling, the two Onsager's relations suggest that the magnon Hall conductivity is an odd function of both the DM interaction and the isotropic exchange coupling. On the other hand, from Eq. (3), an additional $\pi/2$ phase factor in A_{ij} inverts its real and imaginary part and hence leads to $J_{ni,mj}^+ \rightarrow -D_{ni,mj}$ and $D_{ni,mj} \rightarrow J_{ni,mj}^+$. Physically, such a phase factor amounts to rotating the spin frame at either one of the i and j sites around the local z axis by $\pi/2$, which should not generate any measurable difference.

As a concrete example, we consider a ferromagnetic honeycomb lattice with nearest and next nearest exchange coupling, DM interaction and easy-plane anisotropy. The corresponding magnetic Hamiltonian

reads as

$$\begin{aligned} H = - \sum_{\langle i,j \rangle} J_N \mathbf{S}_i \cdot \mathbf{S}_j - \sum_{\langle\langle i,j \rangle\rangle} \sum_{\mu=A,B} J_\mu \mathbf{S}_i^\mu \cdot \mathbf{S}_j^\mu \\ + \sum_{\langle i,j \rangle} D (\mathbf{R}_{ij} \times \hat{z}) \cdot (\mathbf{S}_i \times \mathbf{S}_j). \end{aligned} \quad (12)$$

where \mathbf{R}_{ij} is the unit vector from site i to j . In the nearest neighbor exchange coupling, when $J_A = J_B$, the chiral symmetry $\mathcal{C} = \sigma_x K$ is respected, and the system is hence gapless with vanishing magnon Hall effect. Moreover, an external magnetic field is implied which stabilizes the in-plane ferromagnetic order, as shown in Fig. 2(a).

In Fig. 2(b), we plot the Hall conductivity as a function of J_N and D , with $J_N^2 + D^2$ fixed. We find that κ_{xy} has four lobes with alternating signs, resembling the angular dependence of d_{xy} wave. As a result, κ_{xy} is indeed an odd function of J_N and D , consistent with the two Onsager's relations. Such sign-change of the magnon Hall conductivity can potentially be observed in materials with ferromagnetic-antiferromagnetic transition.

The d -wave pattern further suggests the equivalence between J_N and D . To see this, we note that each A site has three nearest-neighbor bonds, which we label by 1, 2, 3, as shown in Fig. 2. The exchanging coupling parameter on each bond forms a two-dimensional vector, with $(J_1, D_1) = (J_N, -D/\sqrt{2})$, $(J_2, D_2) = (J_N, D \cos(\pi/12))$, and $(J_3, D_3) = (J_N, -D \sin(\pi/12))$. A rotation of the local spin frame at site A then interchanges the role of J_i and D_i : $(J_i, D_i) \rightarrow (D_i, -J_i)$ with $i = 1, 2, 3$. More specifically, since κ_{xy} should be unchanged under such rotation of local spin frame, only the relative orientation angles between the three (J_i, D_i) survive. The leading order contribution to κ_{xy} should then has the following pattern: $\kappa_{xy} = A_1(J_1, D_1) \times (J_2, D_2) + A_2(J_1, D_1) \times (J_3, D_3) + A_3(J_2, D_2) \times (J_3, D_3)$, where A_i is a function of the magnitude of the three vectors (J_ℓ, D_ℓ) , and the cross product of two two-dimensional vector generates a pseudoscalar. Therefore, κ_{xy} is a function of $J_N \cdot D$, consistent with the d -wave pattern and clearly demonstrates the equivalence between J_N and D . Moreover, since $|D_i| < D$, $J_i^2 + D_i^2$ is always slimmer in the D -direction, as can be observed in Fig. 2(b).

Another consequence of the two Onsager's relations is that the DM interaction is not necessary for the magnon Hall effect. It can be fully replaced by the anisotropic exchange coupling. By setting $D = 0$, Eq. (10) suggests that κ is an odd function of the anisotropic exchange parameter Γ . Moreover, similar to the equivalence between D and J^+ , for the anisotropic exchange coupling, the off-diagonal part $\Gamma_{ni,mj}$ is equivalent to $J_{ni,mj}^-$, due to a rotation of the local spin frame at either i or j by $\pi/2$.

To show this, we consider the following ferromagnetic honeycomb model with the magnetic order being along

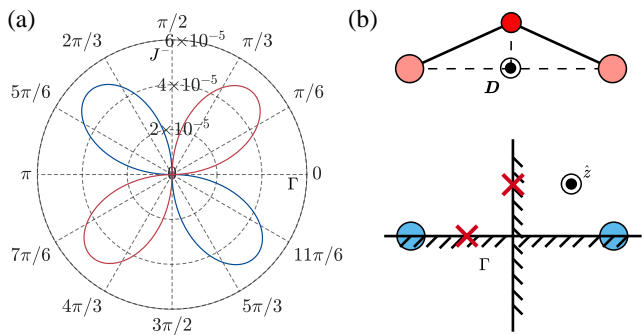


FIG. 3. (a) The thermal conductivity as a function of Γ and J^- . Parameters are $J^+ = \pm 0.5J_0$ which changes sign as Γ varies, $\sqrt{(J^-)^2 + \Gamma^2} = 0.1J_0$, $J_A = 0.05J_0$, and $J_B = 0.075J_0$. The blue and red curve are positive and negative, respectively. (b) Symmetry requirements for DM interaction(top) and anisotropic exchange coupling(bottom).

z -axis:

$$H = \sum_{\langle i,j \rangle} \mathbf{S}_i^T \mathcal{J}_{ij} \mathbf{S}_j - \sum_{\langle\langle i,j \rangle\rangle} \sum_{\mu=A,B} J_\mu \mathbf{S}_i^\mu \cdot \mathbf{S}_j^\mu, \quad (13)$$

where

$$\mathcal{J}_{ij} = \begin{pmatrix} -J^+ + J^- & w_{ij}\Gamma & 0 \\ w_{ij}\Gamma & -J^+ - J^- & 0 \\ 0 & 0 & -J_0 \end{pmatrix}. \quad (14)$$

where Γ , J^+ and J^- are constants representing off-diagonal anisotropic, isotropic, diagonal anisotropic exchange couplings, respectively. w_{ij} are weighing factors for the three nearest-neighbor bonds, and they are chosen to break the in-plane mirror symmetry. The next nearest neighbor term is added to break the chiral symmetry as before.

In Fig. 3 we plot the thermal Hall conductivity as a function of Γ and J^- . One can find a similar d -wave pattern, showing that κ_{xy} is an odd function of both Γ and J^- , and the equivalence between Γ and J^- . We shall emphasize that the anisotropic exchange coupling only affects J^- and Γ in our case, while the one in previous study[7] also serves as antisymmetric exchange interaction in the magnon Hamiltonian[35]. Therefore, our work unambiguously demonstrates that the anisotropic exchange alone can support the magnon Hall effect.

The anisotropic exchange coupling has completely different symmetry requirements from the DM interaction. The latter requires the breaking of inversion symmetry. In comparison, the former requires the breaking of mirror-x and mirror-y symmetry; the inversion symmetry can be retained. This then extends the material candidate for the magnon Hall effect.

We acknowledge useful discussions with Shiyue Deng, Shu Li and Qingtao Zhao. This work is supported by the National Natural Science Foundation of China

(12234017). Y. G. is also supported by the Innovation Program for Quantum Science and Technology (2021ZD0302802). The supercomputing service of USTC is gratefully acknowledged.

* Correspondence author: ygao87@ustc.edu.cn

- [1] H. Katsura, N. Nagaosa, and P. A. Lee, Theory of the thermal hall effect in quantum magnets, *Phys. Rev. Lett.* **104**, 066403 (2010).
- [2] R. Matsumoto and S. Murakami, Theoretical prediction of a rotating magnon wave packet in ferromagnets, *Phys. Rev. Lett.* **106**, 197202 (2011).
- [3] Y. Onose, T. Ideue, H. Katsura, Y. Shiomi, N. Nagaosa, and Y. Tokura, Observation of the magnon hall effect, *Science* **329**, 297 (2010), <https://www.science.org/doi/pdf/10.1126/science.1188260>.
- [4] A. Mook, J. Henk, and I. Mertig, Thermal hall effect in noncollinear coplanar insulating antiferromagnets, *Phys. Rev. B* **99**, 014427 (2019).
- [5] R. Matsumoto and S. Murakami, Rotational motion of magnons and the thermal hall effect, *Phys. Rev. B* **84**, 184406 (2011).
- [6] R. Matsumoto, R. Shindou, and S. Murakami, Thermal hall effect of magnons in magnets with dipolar interaction, *Phys. Rev. B* **89**, 054420 (2014).
- [7] R. R. Neumann, A. Mook, J. Henk, and I. Mertig, Thermal hall effect of magnons in collinear antiferromagnetic insulators: Signatures of magnetic and topological phase transitions, *Phys. Rev. Lett.* **128**, 117201 (2022).
- [8] F. Zhuo, H. Li, and A. Manchon, Topological phase transition and thermal hall effect in kagome ferromagnets, *Phys. Rev. B* **104**, 144422 (2021).
- [9] S. A. Owerre, Topological honeycomb magnon Hall effect: A calculation of thermal Hall conductivity of magnetic spin excitations, *Journal of Applied Physics* **120**, 043903 (2016), https://pubs.aip.org/aip/jap/article-pdf/doi/10.1063/1.4959815/15183579/043903_1_online.pdf.
- [10] S. A. Owerre, Magnon hall effect in ab-stacked bilayer honeycomb quantum magnets, *Phys. Rev. B* **94**, 094405 (2016).
- [11] S. A. Owerre, Topological thermal hall effect in frustrated kagome antiferromagnets, *Phys. Rev. B* **95**, 014422 (2017).
- [12] A. Mook, J. Henk, and I. Mertig, Magnon hall effect and topology in kagome lattices: A theoretical investigation, *Phys. Rev. B* **89**, 134409 (2014).
- [13] X. Cao, K. Chen, and D. He, Magnon hall effect on the lieb lattice, *Journal of Physics: Condensed Matter* **27**, 166003 (2015).
- [14] P. Laurell and G. A. Fiete, Magnon thermal hall effect in kagome antiferromagnets with dzyaloshinskii-moriya interactions, *Phys. Rev. B* **98**, 094419 (2018).
- [15] S. Li and A. H. Nevidomskyy, Topological weyl magnons and thermal hall effect in layered honeycomb ferromagnets, *Phys. Rev. B* **104**, 104419 (2021).
- [16] M. Kawano and C. Hotta, Thermal hall effect and topological edge states in a square-lattice antiferromagnet, *Phys. Rev. B* **99**, 054422 (2019).
- [17] X. Zhang, Y. Zhang, S. Okamoto, and D. Xiao, Thermal hall effect induced by magnon-phonon interactions, *Phys.*

- Rev. Lett. **123**, 167202 (2019).
- [18] L. Onsager, Reciprocal Relations in Irreversible Processes. I., *Physical Review* **37**, 405 (1931).
- [19] L. Onsager, Reciprocal Relations in Irreversible Processes. II., *Physical Review* **38**, 2265 (1931).
- [20] N. Nagaosa, J. Sinova, S. Onoda, A. H. MacDonald, and N. P. Ong, Anomalous hall effect, *Rev. Mod. Phys.* **82**, 1539 (2010).
- [21] I. Dzyaloshinsky, A thermodynamic theory of “weak” ferromagnetism of antiferromagnetics, *Journal of Physics and Chemistry of Solids* **4**, 241 (1958).
- [22] T. Moriya, Anisotropic superexchange interaction and weak ferromagnetism, *Phys. Rev.* **120**, 91 (1960).
- [23] R. Cheng, S. Okamoto, and D. Xiao, Spin nernst effect of magnons in collinear antiferromagnets, *Phys. Rev. Lett.* **117**, 217202 (2016).
- [24] L. Shekhtman, O. Entin-Wohlman, and A. Aharony, Moriya’s anisotropic superexchange interaction, frustration, and dzyaloshinsky’s weak ferromagnetism, *Phys. Rev. Lett.* **69**, 836 (1992).
- [25] D. Wang, X. Bo, F. Tang, and X. Wan, First-principles study of the spin-orbit coupling contribution to anisotropic magnetic interactions, *Phys. Rev. B* **108**, 085140 (2023).
- [26] P. Liu, J. Li, J. Han, X. Wan, and Q. Liu, Spin-group symmetry in magnetic materials with negligible spin-orbit coupling, *Phys. Rev. X* **12**, 021016 (2022).
- [27] L. Šmejkal, J. Sinova, and T. Jungwirth, Beyond conventional ferromagnetism and antiferromagnetism: A phase with nonrelativistic spin and crystal rotation symmetry, *Phys. Rev. X* **12**, 031042 (2022).
- [28] X. Chen, J. Ren, Y. Zhu, Y. Yu, A. Zhang, P. Liu, J. Li, Y. Liu, C. Li, and Q. Liu, Enumeration and representation theory of spin space groups, *Phys. Rev. X* **14**, 031038 (2024).
- [29] Z. Xiao, J. Zhao, Y. Li, R. Shindou, and Z.-D. Song, Spin space groups: Full classification and applications, *Phys. Rev. X* **14**, 031037 (2024).
- [30] Y. Jiang, Z. Song, T. Zhu, Z. Fang, H. Weng, Z.-X. Liu, J. Yang, and C. Fang, Enumeration of spin-space groups: Toward a complete description of symmetries of magnetic orders, *Phys. Rev. X* **14**, 031039 (2024).
- [31] P. A. McClarty and J. G. Rau, Landau theory of altermagnetism, *Phys. Rev. Lett.* **132**, 176702 (2024).
- [32] X. Chen, Y. Liu, P. Liu, Y. Yu, J. Ren, J. Li, A. Zhang, and Q. Liu, *Catalog of unconventional magnons in collinear magnets* (2024), arXiv:2307.12366 [cond-mat.mtrl-sci].
- [33] A. Corticelli, R. Moessner, and P. A. McClarty, Spin-space groups and magnon band topology, *Phys. Rev. B* **105**, 064430 (2022).
- [34] T. Holstein and H. Primakoff, Field dependence of the intrinsic domain magnetization of a ferromagnet, *Phys. Rev.* **58**, 1098 (1940).
- [35] See supplemental material for the derivation of (i)matrix form of spin hamiltonian; (ii)gauge freedom of choosing spin-x axis; (iii)operations of effective time reversal symmetry; (iv) proof of two onsager’s relations; (v)details of hamiltonian of two honeycomb models; (vi) antisymmetric interaction contributed by symmetry anisotropic interaction, .
- [36] J. Colpa, Diagonalization of the quadratic boson hamiltonian, *Physica A: Statistical Mechanics and its Applications* **93**, 327 (1978).
- [37] S. Toth and B. Lake, Linear spin wave theory for single-q incommensurate magnetic structures, *Journal of Physics: Condensed Matter* **27**, 166002 (2015).
- [38] R. Shindou, R. Matsumoto, S. Murakami, and J.-i. Ohe, Topological chiral magnonic edge mode in a magnonic crystal, *Phys. Rev. B* **87**, 174427 (2013).
- [39] A. Okamoto and S. Murakami, Berry curvature for magnons in ferromagnetic films with dipole-exchange interactions, *Phys. Rev. B* **96**, 174437 (2017).
- [40] L. Landau, J. Bell, M. Kearsley, L. Pitaevskii, E. Lifshitz, and J. Sykes, *Electrodynamics of Continuous Media*, COURSE OF THEORETICAL PHYSICS (Elsevier Science, 2013).
- [41] H. Chen, Q. Niu, and A. H. MacDonald, Anomalous hall effect arising from noncollinear antiferromagnetism, *Phys. Rev. Lett.* **112**, 017205 (2014).
- [42] M.-T. Suzuki, T. Koretsune, M. Ochi, and R. Arita, Cluster multipole theory for anomalous hall effect in antiferromagnets, *Phys. Rev. B* **95**, 094406 (2017).

Supplemental material for “Full Onsager’s Relation in Magnon Hall Effect and Its Implication”

Jikun Zhou,¹ Yang Gao,^{1,2} and Qian Niu^{1,2}

¹*CAS Key Laboratory of Strongly-Coupled Quantum Matter Physics and Department of Physics, University of Science and Technology of China, Hefei, Anhui 230026, China*

²*Hefei National Laboratory, University of Science and Technology of China, Hefei 230088, China*

(Dated: January 14, 2025)

I. MATRIX FORM OF GENERALIZED HEISENBERG HAMILTONIAN

In this section, we will derive the matrix element of local spin Hamiltonian in detail. Consider a generalized Heisenberg Hamiltonian

$$H = \frac{1}{2} \sum_{n,m} \sum_{i,j} \sum_{ab} \mathbf{S}_{n,i}^a J_{ni,mj}^{ab} \mathbf{S}_{m,j}^b, \quad (\text{S1})$$

and we only care about bilinear terms so that interaction tensor $J_{ni,mj}$ will have the form

$$J_{ni,mj} = \begin{bmatrix} J_{ni,mj}^{xx} & J_{ni,mj}^{xy} & 0 \\ J_{ni,mj}^{yx} & J_{ni,mj}^{yy} & 0 \\ 0 & 0 & J_{ni,mj}^z \end{bmatrix}. \quad (\text{S2})$$

Thus we can expand Eq. (S1) and use definition of ladder operators $S_{n,i}^{\pm} = S_{n,i}^x \pm iS_{n,i}^y$,

$$\begin{aligned} H &= \frac{1}{2} \sum_{n,m} \sum_{i,j} (S_{n,i}^x, S_{n,i}^y, S_{n,i}^z) \begin{bmatrix} J_{ni,mj}^{xx} & J_{ni,mj}^{xy} & 0 \\ J_{ni,mj}^{yx} & J_{ni,mj}^{yy} & 0 \\ 0 & 0 & J_{ni,mj}^z \end{bmatrix} \begin{pmatrix} S_{m,j}^x \\ S_{m,j}^y \\ S_{m,j}^z \end{pmatrix} \\ &= \frac{1}{2} \sum_{n,m} \sum_{i,j} J_{ni,mj}^{xx} S_{n,i}^x S_{m,j}^x + J_{ni,mj}^{yy} S_{n,i}^y S_{m,j}^y + J_{ni,mj}^{xy} S_{n,i}^x S_{m,j}^y + J_{ni,mj}^{yx} S_{n,i}^y S_{m,j}^x + J_{ni,mj}^{zz} S_{n,i}^z S_{m,j}^z \\ &= \frac{1}{2} \sum_{n,m} \sum_{i,j} \left\{ J_{ni,mj}^{xx} \frac{S_{n,i}^+ + S_{n,i}^-}{2} \frac{S_{m,j}^+ + S_{m,j}^-}{2} + J_{ni,mj}^{yy} \frac{S_{n,i}^+ - S_{n,i}^-}{2i} \frac{S_{m,j}^+ - S_{m,j}^-}{2i} \right. \\ &\quad \left. + J_{ni,mj}^{xy} \frac{S_{n,i}^+ + S_{n,i}^-}{2} \frac{S_{m,j}^+ - S_{m,j}^-}{2i} + J_{ni,mj}^{yx} \frac{S_{n,i}^+ - S_{n,i}^-}{2i} \frac{S_{m,j}^+ + S_{m,j}^-}{2} \right\} + J_{ni,mj}^{zz} S_{n,i}^z S_{m,j}^z \\ &= \frac{1}{2} \sum_{n,m} \sum_{i,j} \frac{1}{4} \left\{ [J_{ni,mj}^{xx} - J_{ni,mj}^{yy} - i(J_{ni,mj}^{xy} + J_{ni,mj}^{yx})] S_{n,i}^+ S_{m,j}^+ + [J_{ni,mj}^{xx} + J_{ni,mj}^{yy} + i(J_{ni,mj}^{xy} - J_{ni,mj}^{yx})] S_{n,i}^+ S_{m,j}^- \right. \\ &\quad \left. + [J_{ni,mj}^{xx} + J_{ni,mj}^{yy} - i(J_{ni,mj}^{xy} - J_{ni,mj}^{yx})] S_{n,i}^- S_{m,j}^+ + [J_{ni,mj}^{xx} - J_{ni,mj}^{yy} + i(J_{ni,mj}^{xy} + J_{ni,mj}^{yx})] S_{n,i}^- S_{m,j}^- \right\} \\ &\quad + J_{ni,mj}^{zz} S_{n,i}^z S_{m,j}^z. \end{aligned} \quad (\text{S3})$$

By the means of Holstein-Primakoff transformation[S1]

$$S_{n,i}^+ \approx \sqrt{2S} a_{n,i}, \quad S_{n,i}^- \approx \sqrt{2S} a_{n,i}^\dagger, \quad S_{n,i}^z = S - a_{n,i}^\dagger a_{n,i}, \quad (\text{S4})$$

Hamiltonian can be turned into

$$\begin{aligned}
H = \frac{S}{2} \sum_{n,m} \sum_{i,j} \frac{1}{2} \left\{ [J_{ni,mj}^{xx} - J_{ni,mj}^{yy} - i(J_{ni,mj}^{xy} + J_{ni,mj}^{yx})] a_{n,i} a_{m,j} + [J_{ni,mj}^{xx} + J_{ni,mj}^{yy} + i(J_{ni,mj}^{xy} - J_{ni,mj}^{yx})] a_{n,i} a_{m,j}^\dagger \right. \\
+ [J_{ni,mj}^{xx} + J_{ni,mj}^{yy} - i(J_{ni,mj}^{xy} - J_{ni,mj}^{yx})] a_{n,i}^\dagger a_{m,j} + [J_{ni,mj}^{xx} - J_{ni,mj}^{yy} + i(J_{ni,mj}^{xy} + J_{ni,mj}^{yx})] a_{n,i}^\dagger a_{m,j}^\dagger \left. \right\} \\
- J_{ni,mj}^{zz} (a_{n,i}^\dagger a_{n,i} + a_{m,j}^\dagger a_{m,j}).
\end{aligned} \tag{S5}$$

Through Fourier transform of creation and annihilation operators: $a_{n,i} = (1/\sqrt{N}) \sum_{\mathbf{k}} e^{i\mathbf{k}\cdot(\mathbf{R}_n + \mathbf{r}_i)} a_{i,\mathbf{k}}$ and $a_{n,i}^\dagger = (1/\sqrt{N}) \sum_{\mathbf{k}} e^{-i\mathbf{k}\cdot(\mathbf{R}_n + \mathbf{r}_i)} a_{i,\mathbf{k}}^\dagger$, we get Hamiltonian in momentum space

$$\begin{aligned}
H = \frac{S}{2} \sum_{n,m} \sum_{i,j} \frac{1}{2} \left\{ [J_{ni,mj}^{xx} - J_{ni,mj}^{yy} - i(J_{ni,mj}^{xy} + J_{ni,mj}^{yx})] e^{-i\mathbf{k}\cdot(\mathbf{R}_{mj} - \mathbf{R}_{ni})} a_{i,\mathbf{k}} a_{j,-\mathbf{k}} \right. \\
+ [J_{ni,mj}^{xx} + J_{ni,mj}^{yy} + i(J_{ni,mj}^{xy} - J_{ni,mj}^{yx})] e^{-i\mathbf{k}\cdot(\mathbf{R}_{mj} - \mathbf{R}_{ni})} a_{i,\mathbf{k}} a_{j,\mathbf{k}}^\dagger \\
+ [J_{ni,mj}^{xx} + J_{ni,mj}^{yy} - i(J_{ni,mj}^{xy} - J_{ni,mj}^{yx})] e^{i\mathbf{k}\cdot(\mathbf{R}_{mj} - \mathbf{R}_{ni})} a_{i,\mathbf{k}}^\dagger a_{j,\mathbf{k}} \\
\left. + [J_{ni,mj}^{xx} - J_{ni,mj}^{yy} + i(J_{ni,mj}^{xy} + J_{ni,mj}^{yx})] e^{i\mathbf{k}\cdot(\mathbf{R}_{mj} - \mathbf{R}_{ni})} a_{i,\mathbf{k}}^\dagger a_{j,-\mathbf{k}}^\dagger \right\} - J_{ni,mj}^{zz} (a_{i,\mathbf{k}}^\dagger a_{i,\mathbf{k}} + a_{j,\mathbf{k}}^\dagger a_{j,\mathbf{k}}).
\end{aligned} \tag{S6}$$

Finally, we can turn this Hamiltonian to matrix form by choosing basis $\psi_{\mathbf{k}} = (a_{1,\mathbf{k}}, \dots, a_{N,\mathbf{k}}, a_{1,-\mathbf{k}}^\dagger, \dots, a_{N,-\mathbf{k}}^\dagger)^T$,

$$H = \sum_{\mathbf{k}} \psi_{\mathbf{k}}^\dagger \mathcal{H}_{\mathbf{k}} \psi_{\mathbf{k}} = \sum_{\mathbf{k}} \psi_{\mathbf{k}}^\dagger \frac{S}{2} \begin{bmatrix} \mathbf{A}(\mathbf{k}) & \mathbf{B}(\mathbf{k}) \\ \mathbf{B}^*(-\mathbf{k}) & \mathbf{A}^*(-\mathbf{k}) \end{bmatrix} \psi_{\mathbf{k}}. \tag{S7}$$

And we have shown that, submatrices $\mathbf{A}(\mathbf{k})$ and $\mathbf{B}(\mathbf{k})$ are[S2]

$$\begin{aligned}
[\mathbf{A}(\mathbf{k})]_{i,j} &= \sum_{m,n} \frac{1}{2} [J_{ni,mj}^{xx} + J_{ni,mj}^{yy} - i(J_{ni,mj}^{xy} - J_{ni,mj}^{yx})] e^{i\mathbf{k}\cdot(\mathbf{R}_{mj} - \mathbf{R}_{ni})} - \delta_{ij} \sum_{\ell} J_{nm}^{iz,\ell z}, \\
[\mathbf{B}(\mathbf{k})]_{i,j} &= \sum_{m,n} \frac{1}{2} [J_{ni,mj}^{xx} - J_{ni,mj}^{yy} + i(J_{ni,mj}^{xy} + J_{ni,mj}^{yx})] e^{i\mathbf{k}\cdot(\mathbf{R}_{mj} - \mathbf{R}_{ni})}.
\end{aligned} \tag{S8}$$

By denoting $J_{ni,mj}^{xx} + J_{ni,mj}^{yy} \rightarrow J_{ni,mj}^+$, $J_{ni,mj}^{xx} - J_{ni,mj}^{yy} \rightarrow J_{ni,mj}^-$, $J_{ni,mj}^{xy} - J_{ni,mj}^{yx} \rightarrow D_{ni,mj}$, $J_{ni,mj}^{xy} + J_{ni,mj}^{yx} \rightarrow \Gamma_{ni,mj}$, we finally arrive at Eq.(3) in main text

$$\begin{aligned}
A_{ij}(\mathbf{k}) &= \sum_{m,n} \frac{1}{2} (J_{ni,mj}^+ - iD_{ni,mj}) e^{i\mathbf{k}\cdot(\mathbf{R}_{mj} - \mathbf{R}_{ni})} - \delta_{ij} \sum_{mnl} J_{ni,m\ell}^{zz}, \\
B_{ij}(\mathbf{k}) &= \sum_{m,n} \frac{1}{2} (J_{ni,mj}^- + i\Gamma_{ni,mj}) e^{i\mathbf{k}\cdot(\mathbf{R}_{mj} - \mathbf{R}_{ni})}.
\end{aligned} \tag{S9}$$

II. GAUGE FREEDOM OF CHOOSING SPIN-X DIRECTION

At each site in a unit cell, only the spin-z direction is well-defined, and any direction perpendicular to the z -th direction can equally serve as the x direction. This introduces a gauge freedom in selecting the spin-x axis. However, this gauge transformation does not impact physical results, such as the Berry curvature.

Consider an initial local coordinate system with axes x , y and z , where the z -axis aligns with the orientation of the local magnetization, while x and y are chosen arbitrarily. If we rotate this coordinate system counterclockwise around z -axis by an angle θ , we obtain a new coordinate system x', y', z as shown in Fig.S1.

New spin components and original ones are related by rotation matrix

$$\begin{pmatrix} S_{x'} \\ S_{y'} \end{pmatrix} = \begin{pmatrix} \cos \theta & -\sin \theta \\ \sin \theta & \cos \theta \end{pmatrix} \begin{pmatrix} S_x \\ S_y \end{pmatrix} \tag{S10}$$

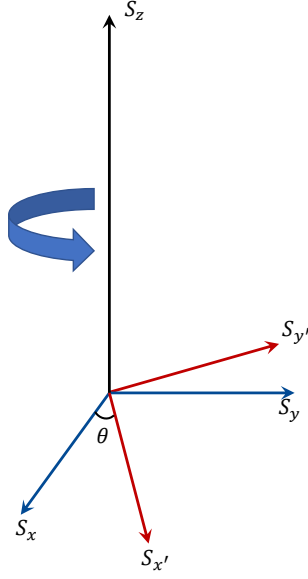


FIG. S1. Rotation of local coordinate. S_x, S_y, S_z correspond to original local spin system while $S_{x'}, S_{y'}, S_z$ represent the new one.

Thus new ladder operator $S^{+'}$ is

$$\begin{aligned}
 S^{+'} &= S_{x'} + iS_{y'} \\
 &= (S_x \cos \theta - S_y \sin \theta) + i(S_x \sin \theta + S_y \cos \theta) \\
 &= (\cos \theta + i \sin \theta) (S_x + iS_y) \\
 &= e^{i\theta} S^+
 \end{aligned} \tag{S11}$$

Similarly, $S^{-'} = e^{-i\theta} S^-$. The new ladder operators differ from the original ones by a phase factor that depends on the rotation angle. Consequently, the creation and annihilation operators are also modified by this phase factor according to Holstein-Primakoff transformation. Rotating the local coordinate of each sublattice by different angles is equivalent to applying a gauge transformation on the basis $\psi'_{\mathbf{k}} = \mathcal{P}\psi_{\mathbf{k}}$, where $\mathcal{P} = \text{diag}(e^{i\theta_1}, \dots, e^{i\theta_N}, e^{-i\theta_1}, \dots, e^{-i\theta_N})$. Then Hamiltonian will be transformed into

$$H = \sum_{\mathbf{k}} \psi_{\mathbf{k}}^\dagger \mathcal{P}^\dagger \mathcal{H}_{\mathbf{k}} \mathcal{P} \psi_{\mathbf{k}}. \tag{S12}$$

As a result of this gauge transformation, the new Hamiltonian elements become $A_{ij} e^{i(\theta_i - \theta_j)}$ and $B_{ij} e^{i(\theta_i - \theta_j)}$.

Due to $\mathcal{P}\mathcal{P}^\dagger = \mathbb{I}_{2N}$ with \mathbb{I}_{2N} being $2N \times 2N$ identity, we can demonstrate that the transformed Hamiltonian $\mathcal{P}^\dagger \mathcal{H}_{\mathbf{k}} \mathcal{P}$ can be diagonalized by $\mathcal{P}^\dagger T_{\mathbf{k}}$,

$$T_{\mathbf{k}}^\dagger \mathcal{H}_{\mathbf{k}} T_{\mathbf{k}} = (\mathcal{P}^\dagger T_{\mathbf{k}})^\dagger \mathcal{P}^\dagger \mathcal{H}_{\mathbf{k}} \mathcal{P} (\mathcal{P}^\dagger T_{\mathbf{k}}) = \begin{bmatrix} E_{\mathbf{k}} & \\ & E_{-\mathbf{k}} \end{bmatrix}. \tag{S13}$$

Thus the new Berry Curvature[S3] is

$$\begin{aligned}
 (\Omega_{\mu\nu})'_{n,\mathbf{k}} &= i\epsilon_{\mu\nu} \left[\Sigma_z \frac{\partial (\mathcal{P}^\dagger T_{\mathbf{k}})^\dagger}{\partial k_\mu} \Sigma_z \frac{\partial (\mathcal{P}^\dagger T_{\mathbf{k}})}{\partial k_\nu} \right]_{nn}, \\
 &= i\epsilon_{\mu\nu} \left[\Sigma_z \frac{\partial T_{\mathbf{k}}^\dagger}{\partial k_\mu} \mathcal{P} \Sigma_z \mathcal{P}^\dagger \frac{\partial T_{\mathbf{k}}}{\partial k_\nu} \right]_{nn}, \\
 &= i\epsilon_{\mu\nu} \left[\Sigma_z \frac{\partial T_{\mathbf{k}}^\dagger}{\partial k_\mu} \Sigma_z \frac{\partial T_{\mathbf{k}}}{\partial k_\nu} \right]_{nn}, \\
 &= (\Omega_{\mu\nu})_{n,\mathbf{k}},
 \end{aligned} \tag{S14}$$

where we have used $\mathcal{P}\Sigma_z\mathcal{P}^\dagger = \Sigma_z$ because they are all diagonal matrices. Thus, the Berry curvature remains unchanged under this gauge transformation, and, consequently, the thermal conductivity is also unaffected. Although additional phase factors are introduced into the Hamiltonian elements, they do not alter the physical results. However, as we will discuss in Sec.IV B, they do change our perspective on the structures of thermal conductivity.

III. EFFECTIVE TIME REVERSAL OPERATION \mathcal{T}_x AND \mathcal{T}_y

The full time-reversal symmetry group \tilde{G} allows for different choices of C_2 spin rotations on different sublattice sites. Besides using $\mathcal{T}_x = TC_{2x}^s$ as effective time reversal symmetry[S4–S6] on every site, choosing $\mathcal{T}_y = TC_{2y}^s$ as local effective time reversal symmetry on any sublattice is permitted. \mathcal{T}_y transforms creation and annihilation operators $a_{n,i}(a_{n,i}^\dagger)$ into $a_{n,i}(a_{n,i}^\dagger)$ rather than $-a_{n,i}(-a_{n,i}^\dagger)$ which are transformed by \mathcal{T}_x . This can be shown by performing effective time reversal symmetry operations on ladder operators,

$$\begin{aligned}\mathcal{T}_x S_{n,i}^\pm &= TC_{2x}^s (S_{n,i}^x \pm iS_{n,i}^y) \\ &= -(S_{n,i}^x \pm iS_{n,i}^y) \\ &= -S_{n,i}^\pm,\end{aligned}\tag{S15}$$

while \mathcal{T}_y is different

$$\begin{aligned}\mathcal{T}_y S_{n,i}^\pm &= TC_{2y}^s (S_{n,i}^x \pm iS_{n,i}^y) \\ &= S_{n,i}^x \pm iS_{n,i}^y \\ &= S_{n,i}^\pm.\end{aligned}\tag{S16}$$

It is easy to observe that \mathcal{T}_x will introduce an additional minus sign to the basis function. Thus $\mathcal{T}_x, \mathcal{T}_y$ can be identified as $-K$ and K respectively where K is complex conjugation. Furthermore, under the operations of \mathcal{T}_x and \mathcal{T}_y , the momentum space basis $a_{i,\mathbf{k}}$ transforms to $-a_{i,-\mathbf{k}}$ and $a_{i,-\mathbf{k}}$, respectively. Now we define their operation on momentum space Hamiltonian $\mathcal{H}_{\mathbf{k}}$

$$\begin{aligned}\mathcal{T}_{x(y)}\mathcal{H}_{\mathbf{k}}\mathcal{T}_{x(y)}^{-1} &= \mathcal{T}_{x(y)}e^{-i\mathbf{k}\cdot\mathbf{r}}He^{i\mathbf{k}\cdot\mathbf{r}}\mathcal{T}_{x(y)}^{-1}, \\ &= e^{i\mathbf{k}\cdot\mathbf{r}}H^*e^{-i\mathbf{k}\cdot\mathbf{r}}, \\ &= \mathcal{H}_{-\mathbf{k}}^*.\end{aligned}\tag{S17}$$

According to Hamiltonian element in Eq.(S9), applying complex conjugation along with transformation $\mathbf{k} \rightarrow -\mathbf{k}$ leaves momentum \mathbf{k} unchanged

$$\begin{aligned}A_{ij}^*(-\mathbf{k}) &= \sum_{m,n} \frac{1}{2} (J_{ni,mj}^+ + iD_{ni,mj})e^{i\mathbf{k}\cdot(\mathbf{R}_{mj}-\mathbf{R}_{ni})} - \delta_{ij} \sum_{mnl} J_{ni,ml}^{zz}, \\ B_{ij}^*(-\mathbf{k}) &= \sum_{m,n} \frac{1}{2} (J_{ni,mj}^- - i\Gamma_{ni,mj})e^{i\mathbf{k}\cdot(\mathbf{R}_{mj}-\mathbf{R}_{ni})}.\end{aligned}\tag{S18}$$

As a result, parameters coupled with imaginary unit i acquire a minus sign and $\mathcal{H}_{-\mathbf{k}}^*(J_{ij}^\pm, D_{ij}, \Gamma_{ij})$ can be written as $\mathcal{H}_{\mathbf{k}}(J_{ij}^\pm, -D_{ij}, -\Gamma_{ij})$.

IV. PROOF OF ONSAGER'S RELATION

A. First Onsager's Relation

In this part, we aim to determine the relationship between original Berry curvature and its time-reversed counterpart under effective time reversal operation \mathcal{T}_x . Firstly, we replace the original parameter sets $(J_{ij}^\pm, D_{ij}, \Gamma_{ij})$ with new time-reversed parameter sets $(J_{ij}^\pm, -D_{ij}, -\Gamma_{ij})$ as discussed in Sec.III. Then Berry curvature changes as follows:

$$\mathcal{T}_x[(\Omega_{\mu\nu})_{n,\mathbf{k}}(J^\pm, D, \Gamma)]\mathcal{T}_x^{-1} = (\Omega_{\mu\nu})_{n,\mathbf{k}}(J^\pm, -D, -\Gamma).\tag{S19}$$

For simplicity, we omit the subscripts ni, mj here. Alternatively, we may consider the effect of \mathcal{T}_x on the wave function itself, leading to the following transformation

$$\begin{aligned} \mathcal{T}_x[(\Omega_{\mu\nu})_{n,\mathbf{k}}(J^\pm, D, \Gamma)]\mathcal{T}_x^{-1} &= i\epsilon_{\mu\nu} \left\{ \Sigma_z \frac{\partial [T_{-\mathbf{k}}^*(J^\pm, D, \Gamma)]^\dagger}{\partial k_\mu} \Sigma_z \frac{\partial T_{-\mathbf{k}}^*(J^\pm, D, \Gamma)}{\partial k_\nu} \right\}_{nn}, \\ &= i\epsilon_{\mu\nu} \left\{ \Sigma_z \frac{\partial T_{-\mathbf{k}}^T(J^\pm, D, \Gamma)}{\partial k_\mu} \Sigma_z \frac{\partial T_{-\mathbf{k}}^*(J^\pm, D, \Gamma)}{\partial k_\nu} \right\}_{nn}. \end{aligned} \quad (\text{S20})$$

Since we are only concerned with the diagonal elements, transposing the matrix does not alter the final result. Thus, we obtain

$$\begin{aligned} \mathcal{T}_x[(\Omega_{\mu\nu})_{n,\mathbf{k}}(J^\pm, D, \Gamma)]\mathcal{T}_x^{-1} &= i\epsilon_{\mu\nu} \left\{ \Sigma_z \frac{\partial T_{-\mathbf{k}}^\dagger(J^\pm, D, \Gamma)}{\partial k_\nu} \Sigma_z \frac{\partial T_{-\mathbf{k}}(J^\pm, D, \Gamma)}{\partial k_\mu} \right\}_{nn}, \\ &= -(\Omega_{\mu\nu})_{n,-\mathbf{k}}(J^\pm, D, \Gamma). \end{aligned} \quad (\text{S21})$$

These two relations lead to the following conclusion

$$(\Omega_{\mu\nu})_{n,\mathbf{k}}(J_{ij}^\pm, D_{ij}, \Gamma_{ij}) = -(\Omega_{\mu\nu})_{n,-\mathbf{k}}(J_{ij}^\pm, -D_{ij}, -\Gamma_{ij}). \quad (\text{S22})$$

Additionally, eigen equation of $\mathcal{H}_{\mathbf{k}}$ reads

$$\Sigma_z \mathcal{H}_{\mathbf{k}}(J^\pm, D, \Gamma) T_{\mathbf{k}}(J^\pm, D, \Gamma) = T_{\mathbf{k}}(J^\pm, D, \Gamma) \begin{bmatrix} E_{\mathbf{k}}(J^\pm, D, \Gamma) & \\ & E_{-\mathbf{k}}(J^\pm, D, \Gamma) \end{bmatrix} \quad (\text{S23})$$

and eigen equation of $\mathcal{H}_{-\mathbf{k}}^*$ is

$$\Sigma_z \mathcal{H}_{-\mathbf{k}}^*(J^\pm, D, \Gamma) T_{-\mathbf{k}}^*(J^\pm, D, \Gamma) = T_{-\mathbf{k}}^*(J^\pm, D, \Gamma) \begin{bmatrix} E_{-\mathbf{k}}(J^\pm, D, \Gamma) & \\ & E_{\mathbf{k}}(J^\pm, D, \Gamma) \end{bmatrix}. \quad (\text{S24})$$

By changing parameter set, we obtain

$$\Sigma_z \mathcal{H}_{\mathbf{k}}(J^\pm, -D, -\Gamma) T_{\mathbf{k}}(J^\pm, -D, -\Gamma) = T_{\mathbf{k}}(J^\pm, D, \Gamma) \begin{bmatrix} E_{\mathbf{k}}(J^\pm, -D, -\Gamma) & \\ & E_{-\mathbf{k}}(J^\pm, -D, -\Gamma) \end{bmatrix}. \quad (\text{S25})$$

Thus energy dispersion satisfies the relation $\varepsilon_{n,\mathbf{k}}(J^\pm, D, \Gamma) = \varepsilon_{n,-\mathbf{k}}(J^\pm, -D, -\Gamma)$. Combining these conclusions, we have

$$\begin{aligned} \kappa_{\mu\nu}(J^\pm, D, \Gamma) &= -\frac{k_B^2 T}{\hbar (2\pi)^2} \sum_{n=1}^N \int c_2 [\rho(\varepsilon_{n,\mathbf{k}}(J^\pm, D, \Gamma))] (\Omega_{\mu\nu})_{n,\mathbf{k}}(J^\pm, D, \Gamma) d^2k, \\ &= -\frac{k_B^2 T}{\hbar (2\pi)^2} \sum_{n=1}^N \int c_2 [\rho(\varepsilon_{n,-\mathbf{k}}(J^\pm, -D, -\Gamma))] [-(\Omega_{\mu\nu})_{n,-\mathbf{k}}(J^\pm, -D, -\Gamma)] d^2k, \\ &= -\kappa_{\mu\nu}(J^\pm, -D, -\Gamma). \end{aligned} \quad (\text{S26})$$

Therefore, the first Onsager's relation for thermal conductivity is

$$\kappa_{\mu\nu}(J_{ij}^\pm, -D_{ij}, -\Gamma_{ij}) = -\kappa_{\mu\nu}(J_{ij}^\pm, D_{ij}, \Gamma_{ij}). \quad (\text{S27})$$

B. Second Onsager's Relation

Now we choose to apply effective time-reversal symmetry in a non-uniform manner. We divide the spins within a unit cell into two groups: the time-reversal operation \mathcal{T}_x acts on spins in the first group, while \mathcal{T}_y acts on spins in the remaining group. The total effective time reversal symmetry is $\mathcal{T} = (-KI_{n_1}) \oplus (KI_{n_2})$ where n_1 and n_2 are the number of spins in these two groups. Accordingly, parameters are separated into two types $(J_{ij}^{\pm, \text{intra}}, D_{ij}^{\text{intra}}, \Gamma_{ij}^{\text{intra}})$ and $(J_{ij}^{\pm, \text{inter}}, D_{ij}^{\text{inter}}, \Gamma_{ij}^{\text{inter}})$. When site i and site j are in the same group, there will not be an extra minus sign after effective time reversal operation. Thus intra-group parameters change as we discussed

in Sec.IV A, $(J_{ij}^{\pm,intra}, D_{ij}^{intra}, \Gamma_{ij}^{intra}) \rightarrow (J_{ij}^{\pm,intra}, -D_{ij}^{intra}, -\Gamma_{ij}^{intra})$. While site i and j belong to different groups, the extra minus sign multiplied with $(\mathcal{H}_{-\mathbf{k}}^*)_{ij}$ given by \mathcal{T} can not be canceled out and new parameter set will be $(-J_{ij}^{\pm,inter}, D_{ij}^{inter}, \Gamma_{ij}^{inter})$ due to this extra minus sign. For example, $\mathcal{T}_{ij} = \mathcal{T}_x^i \otimes \mathcal{T}_y^j$,

$$\begin{aligned}\mathcal{T}_{ij} A_{ij}^{inter}(\mathbf{k}) \mathcal{T}_{ij}^{-1} &= \sum_{m,n} \frac{1}{2} \left(-J_{ni,mj}^{+,inter} - i D_{ni,mj}^{inter} \right) e^{i\mathbf{k} \cdot (\mathbf{R}_{mj} - \mathbf{R}_{ni})}, \\ \mathcal{T}_{ij} B_{ij}^{inter}(\mathbf{k}) \mathcal{T}_{ij}^{-1} &= \sum_{m,n} \frac{1}{2} \left(-J_{ni,mj}^{-,inter} + i \Gamma_{ni,mj}^{inter} \right) e^{i\mathbf{k} \cdot (\mathbf{R}_{mj} - \mathbf{R}_{ni})}.\end{aligned}\tag{S28}$$

Compared with Eq.(S9), $J_{ni,mj}^+$ and $J_{ni,mj}^-$ are inverted. The remainder of the proof follows the same steps as in Sec.IV A, with the only difference being the modified parameter set. Consequently, the second Onsager's relation is

$$\kappa_{\mu\nu}(J_{ij}^{\pm,intra}, -D_{ij}^{intra}, -\Gamma_{ij}^{intra}, -J_{ij}^{\pm,inter}, D_{ij}^{inter}, \Gamma_{ij}^{inter}) = -\kappa_{\mu\nu}(J_{ij}^{\pm,intra}, D_{ij}^{intra}, \Gamma_{ij}^{intra}, J_{ij}^{\pm,inter}, D_{ij}^{inter}, \Gamma_{ij}^{inter}).\tag{S29}$$

Alternatively, we can still use \mathcal{T}_x in the second group but rotate the local coordinates counterclockwise by $\pi/2$ making original y -axis the new x -axis. The phase factor associated with this transform is $e^{i\pi/2}$ which is simply imaginary unit i . This will cause a gauge transform on Hamiltonian as we discussed in Sec.II. The intra-group parameters remain the same because they share the same coordinate, causing the phase factor to cancel out. However, for the inter-group parameters, an additional factor of i appears, so that J_{ij}^{\pm} is now coupled with i , instead of D_{ij} and Γ_{ij} , e.g. $(J_{ij}^+ + iD_{ij}) \rightarrow (iJ_{ij}^+ - D_{ij})$. Under effective times reversal symmetry \mathcal{T}_x as discussed in Sec.IV A, new parameter set will be $(-J_{ij}^{\pm}, D_{ij}, \Gamma_{ij})$. This analysis is consistent with Eq.(S29). We will illustrate this point in detail using the two examples provided in the main text in Sec.V.

V. MATRIX FORM OF HAMILTONIAN IN FERROMAGNETIC HONEYCOMB MODELS

In the first ferromagnetic honeycomb model, the Hamiltonian includes nearest-neighbor and next-nearest-neighbor exchange couplings, as well as DM interactions. The magnetic field term and easy-plane anisotropy are not explicitly included, as they enter the Hamiltonian as constants. Because there are no pairing terms $a_{n,i}^\dagger a_{m,j}^\dagger$ or $a_{n,i} a_{m,j}$, the 4×4 Hamiltonian reduces to 2×2 , namely, we use Nambu basis $\psi_{\mathbf{k}} = (a_{\mathbf{k}}, b_{\mathbf{k}})$ where $a_{\mathbf{k}}$ and $b_{\mathbf{k}}$ are annihilation operators of sublattice A and B respectively. Thus the matrix form of Hamiltonian in first case is

$$\mathcal{H}_{\mathbf{k}} = S \begin{bmatrix} \mathcal{J}_A - J_{Ag}(\mathbf{k}) & -J_N f(\mathbf{k}) - iDh(\mathbf{k}) \\ -J_N f^*(\mathbf{k}) + iDh^*(\mathbf{k}) & \mathcal{J}_B - J_{Bg}(\mathbf{k}) \end{bmatrix},\tag{S30}$$

where $\mathcal{J}_{A(B)} = 3J_N + 6J_{A(B)}$ with $g(\mathbf{k}) = \sum_i \cos(\mathbf{k} \cdot \mathbf{d}_i)$, $f(\mathbf{k}) = \sum_i \exp(i\mathbf{k} \cdot \mathbf{a}_i)$, $h(\mathbf{k}) = \sum_i [(\mathbf{a}_i \times \hat{z}) \cdot \mathbf{m}] \exp(i\mathbf{k} \cdot \mathbf{a}_i)$ with \mathbf{d}_i linking next nearest neighbors, \mathbf{a}_i linking nearest neighbors and $\mathbf{S}_i = S\mathbf{m} = S(\cos 45^\circ, \sin 45^\circ)$ being magnetization in ground state. We denote J_N on the diagonal as J_0 , i.e., $\mathcal{J}_{A(B)} = 3J_0 + 6J_{A(B)}$. This distinction is similar to that in XXZ Heisenberg model.

If we rotate the local coordinate of sublattice B by $\pi/2$ counterclockwise, the gauge transformation discussed in Sec. II will be $\mathcal{P} = \text{diag}(1, i)$. Consequently, the new Hamiltonian is given by

$$\mathcal{P}^\dagger \mathcal{H}_{\mathbf{k}} \mathcal{P} = S \begin{bmatrix} \mathcal{J}_A - J_{Ag}(\mathbf{k}) & -iJ_N f(\mathbf{k}) + Dh(\mathbf{k}) \\ iJ_N f^*(\mathbf{k}) + Dh^*(\mathbf{k}) & \mathcal{J}_B - J_{Bg}(\mathbf{k}) \end{bmatrix}.\tag{S31}$$

Under this transformation, the roles of J_i and D_i are exchanged as : $(J_i, D_i) \rightarrow (D_i, -J_i)$, where i is bond index. From the new Hamiltonian, it is evident that J_N breaks effective time reversal symmetry \mathcal{T}_x and the Onsager's relation will be $\kappa_{xy}(J_N, D) = -\kappa_{xy}(-J_N, D)$.

In the second case, we give an interaction tensor which contains traceless part J^- and symmetric part Γ . These two terms will bring terms $a_{n,i}^\dagger a_{m,j}^\dagger$ and $a_{n,i} a_{m,j}$ and so the Hamiltonian will be 4×4

$$\mathcal{H}_{\mathbf{k}} = \frac{S}{2} \begin{bmatrix} \mathcal{J}_A - J_{Ag}(\mathbf{k}) & -J^+ f(\mathbf{k}) & 0 & J^- f(\mathbf{k}) + i\Gamma l(\mathbf{k}) \\ -J^+ f^*(\mathbf{k}) & \mathcal{J}_B - J_{Bg}(\mathbf{k}) & J^- f^*(\mathbf{k}) + i\Gamma l^*(\mathbf{k}) & 0 \\ 0 & J^- f(\mathbf{k}) - i\Gamma l(\mathbf{k}) & \mathcal{J}_A - J_{Ag}(\mathbf{k}) & -J^+ f^*(\mathbf{k}) \\ J^- f^*(\mathbf{k}) - i\Gamma l^*(\mathbf{k}) & 0 & -J^+ f^*(\mathbf{k}) & \mathcal{J}_B - J_{Bg}(\mathbf{k}) \end{bmatrix}\tag{S32}$$

where definitions of $\mathcal{J}_{A(B)}$, $f(\mathbf{k})$ and $g(\mathbf{k})$ are the same as in the first case. Here, $l(\mathbf{k}) = \sum_i w_{0i} \exp(i\mathbf{k} \cdot \mathbf{a}_i)$ where \mathbf{a}_i are nearest neighbor vectors and w_{0i} are weighing factors for three nearest-neighbor bonds to break in-plane mirror symmetry.

When rotating local coordinate of sublattice B by $\pi/2$ counterclockwise, the gauge transform will be

$$\mathcal{P} = \begin{bmatrix} 1 & & & \\ & i & & \\ & & 1 & \\ & & & -i \end{bmatrix}. \quad (\text{S33})$$

Consequently, Hamiltonian will be transformed to

$$\mathcal{P}^\dagger \mathcal{H}_{\mathbf{k}} \mathcal{P} = \frac{S}{2} \begin{bmatrix} \mathcal{J}_A - J_{Ag}(\mathbf{k}) & -iJ^+ f(\mathbf{k}) & 0 & -iJ^- f(\mathbf{k}) + \Gamma l(\mathbf{k}) \\ iJ^+ f^*(\mathbf{k}) & \mathcal{J}_B - J_{Bg}(\mathbf{k}) & -iJ^- f^*(\mathbf{k}) + \Gamma l^*(\mathbf{k}) & 0 \\ 0 & iJ^- f(\mathbf{k}) + \Gamma l(\mathbf{k}) & \mathcal{J}_A - J_{Ag}(\mathbf{k}) & iJ^+ f^*(\mathbf{k}) \\ iJ^- f^*(\mathbf{k}) + \Gamma l^*(\mathbf{k}) & 0 & -iJ^+ f^*(\mathbf{k}) & \mathcal{J}_B - J_{Bg}(\mathbf{k}) \end{bmatrix}. \quad (\text{S34})$$

In this new Hamiltonian, if we consider \mathcal{T}_x as effective time reversal symmetry acting on both sublattice A and B, only parameters coupled with imaginary unit i , namely J^+ and J^- , will break effective time reversal symmetry. Though Berry curvature remains unchanged, the Onsager's relation is modified to $\kappa_{xy}(J^+, J^-, \Gamma) = -\kappa_{xy}(-J^+, -J^-, \Gamma)$ instead of the original form $\kappa_{xy}(J^+, J^-, \Gamma) = -\kappa_{xy}(J^+, J^-, -\Gamma)$.

VI. DM-LIKE INTERACTION CONTRIBUTED BY SYMMETRIC ANISOTROPIC INTERACTION

In previous study[S7], it was shown that nearest-neighbor bond-dependent anisotropic interaction can induce magnon Hall effect in antiferromagnetic honeycomb lattice. The spin orientations of sublattice A and B of this model are depicted in FIG.S2 where the system is in a coplanar spin-flop phase.

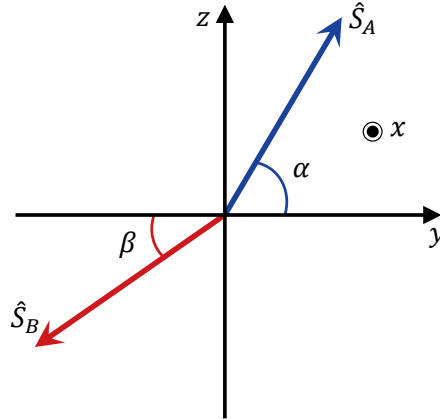


FIG. S2. Spin configuration of coplanar spin-flop phase in [S7].

The spin Hamiltonian mentioned in [S7] between nearest-neighbor sites is given by

$$H_{NN} = \frac{1}{2\hbar^2} \sum_{\langle i,j \rangle} \mathbf{S}_i^T \begin{pmatrix} J + J_a \cos \theta_{ij} & -J_a \sin \theta_{ij} & 0 \\ -J_a \sin \theta_{ij} & J - J_a \cos \theta_{ij} & 0 \\ 0 & 0 & J_z \end{pmatrix} \mathbf{S}_j, \quad (\text{S35})$$

where J is Heisenberg interaction strength and J_a is bond-dependent exchange interaction strength with bond-dependent angle factor θ_{ij} . To transform this model into the local coordinate system, we use a rotation matrix that relates the local and global coordinate systems, as defined in[S6, S8]

$$\mathbf{S}_i = R_i \bar{\mathbf{S}}_i. \quad (\text{S36})$$

In the spin configuration under consideration, if the spin-x axis aligns with the global x-axis, the rotation matrices for sublattices A and B are:

$$R_A = \begin{pmatrix} 1 & 0 & 0 \\ 0 & \sin \alpha & \cos \alpha \\ 0 & -\cos \alpha & \sin \alpha \end{pmatrix}, \quad R_B = \begin{pmatrix} 1 & 0 & 0 \\ 0 & -\sin \beta & -\cos \beta \\ 0 & \cos \beta & -\sin \beta \end{pmatrix} \quad (\text{S37})$$

Substituting these rotation matrices into Eq. (S35), assuming site i belongs to sublattice A, the Hamiltonian becomes:

$$H_{NN} = \frac{1}{2\hbar^2} \sum_{\langle i,j \rangle} \bar{\mathbf{S}}_i^T R_A^T \begin{pmatrix} J + J_a \cos \theta_{ij} & -J_a \sin \theta_{ij} & 0 \\ -J_a \sin \theta_{ij} & J - J_a \cos \theta_{ij} & 0 \\ 0 & 0 & J_z \end{pmatrix} R_B \bar{\mathbf{S}}_j, \quad (\text{S38})$$

From this, the off-diagonal components of the interaction tensor in the local coordinate system are:

$$\begin{aligned} \bar{J}_{xy} &= -J_a \sin \theta_{ij} \sin \beta = -J_a \sin \theta_{ij} \left(\frac{\sin \beta - \sin \alpha}{2} + \frac{\sin \alpha + \sin \beta}{2} \right), \\ \bar{J}_{yx} &= -J_a \sin \theta_{ij} \sin \alpha = -J_a \sin \theta_{ij} \left(\frac{\sin \alpha - \sin \beta}{2} + \frac{\sin \alpha + \sin \beta}{2} \right). \end{aligned} \quad (\text{S39})$$

Thus the antisymmetric part and symmetric part will be

$$\begin{aligned} \bar{J}_{xy} - \bar{J}_{yx} &= -J_a \sin \theta_{ij} (\sin \beta - \sin \alpha), \\ \bar{J}_{xy} + \bar{J}_{yx} &= -J_a \sin \theta_{ij} (\sin \beta + \sin \alpha). \end{aligned} \quad (\text{S40})$$

It is evident that the off-diagonal components are symmetric only when $\sin \alpha = \sin \beta$ which corresponds to collinear cases. Otherwise there is always antisymmetric contribution, which resembles DM interaction in collinear spin configurations.

-
- [S1] T. Holstein and H. Primakoff, Field dependence of the intrinsic domain magnetization of a ferromagnet, *Phys. Rev.* **58**, 1098 (1940).
- [S2] A. Corticelli, R. Moessner, and P. A. McClarty, Spin-space groups and magnon band topology, *Phys. Rev. B* **105**, 064430 (2022).
- [S3] R. Matsumoto, R. Shindou, and S. Murakami, Thermal hall effect of magnons in magnets with dipolar interaction, *Phys. Rev. B* **89**, 054420 (2014).
- [S4] H. Chen, Q. Niu, and A. H. MacDonald, Anomalous hall effect arising from noncollinear antiferromagnetism, *Phys. Rev. Lett.* **112**, 017205 (2014).
- [S5] M.-T. Suzuki, T. Koretsune, M. Ochi, and R. Arita, Cluster multipole theory for anomalous hall effect in antiferromagnets, *Phys. Rev. B* **95**, 094406 (2017).
- [S6] A. Mook, J. Henk, and I. Mertig, Thermal hall effect in noncollinear coplanar insulating antiferromagnets, *Phys. Rev. B* **99**, 014427 (2019).
- [S7] R. R. Neumann, A. Mook, J. Henk, and I. Mertig, Thermal hall effect of magnons in collinear antiferromagnetic insulators: Signatures of magnetic and topological phase transitions, *Phys. Rev. Lett.* **128**, 117201 (2022).
- [S8] P. Laurell and G. A. Fiete, Magnon thermal hall effect in kagome antiferromagnets with dzyaloshinskii-moriya interactions, *Phys. Rev. B* **98**, 094419 (2018).